

# Supplement to “Monopedal Running Control: SLIP Embedding and Virtual Constraint Controllers”

May 4, 2007

## ABSTRACT

This document presents additional results accompanying the paper [1]. The document is divided in two parts. In the first part, details regarding the simulation implementation of the controllers in [1] are given. In the second part, additional results that support the conclusions derived in [1] are included. The reader who is not interested in the implementation part can pass directly to Section II.

## I. IMPLEMENTATION DETAILS

### A. Input Saturation

Including saturation is necessary to have reasonable domain of attraction in the Rigid Target Model controller. The saturation was implemented as follows. The horizontal and vertical ground reaction forces can be computed from the inputs based on the formula,

$$\underbrace{\begin{pmatrix} F_x \\ F_y \end{pmatrix}}_{F_G} = \underbrace{\begin{pmatrix} -\sin(\varphi + \theta) & -\frac{1}{l}\cos(\varphi + \theta) \\ \cos(\varphi + \theta) & -\frac{1}{l}\sin(\varphi + \theta) \end{pmatrix}}_{\mathbf{J}} \underbrace{\begin{pmatrix} u_1 \\ u_2 \end{pmatrix}}_u. \quad (\text{S-1})$$

Let  $\mu$  be the friction coefficient and  $F_y^{\min}$  be the minimum value of the vertical component of the ground reaction (in the simulations included in the paper  $\mu = 0.8$ , and  $F_y^{\min} = 10N$ ). Suppose that the feedback controller requires  $u_1$  and  $u_2$ . Then, based on  $u_1$  and  $u_2$  the corresponding components  $F_x$  and  $F_y$  of the ground reaction force  $F_G$  can be computed via (S-1).

1. If  $F_y \leq F_y^{\min}$ , then set  $F_y = F_y^{\min}$  and compute  $F_x = \mu|F_y| = \mu|F_y^{\min}|$ . Then, using (S-1), compute  $u = \mathbf{J}^{-1}F_G$  and use the result as the input.

2. If  $F_y > F_y^{\min}$  and  $\mu < F_x/|F_y|$  (i.e. if sliding occurs) set  $F_x = \mu|F_y|$ . Then, using (S-1), compute  $u = \mathbf{J}^{-1}F_G$  and use the result as the input.

These conditions imposed on the inputs  $u_1$  and  $u_2$  guarantee that, neither the unilateral ground force nor the friction limitation constraint is violated.

### B. Designing the Target Model and Virtual Holonomic Constraints

In this section, details regarding the design of holonomic constraints for suitably parameterizing the zero dynamics of both the SLIP embedding controller and the Rigid Target Model controller are described.

#### B1) Designing the Target Model in the SLIP embedding controller:

As was mentioned in [1], the SLIP embedding controller introduces a number of parameters in the stance phase dynamics associated with properties of the target model that are to be chosen via optimization. According to the notation in [1], the array  $\alpha_s = (\bar{\theta}, k, r_0, \Delta r)'$  includes the physical properties of the target model i.e. the SLIP as well as the desired pitch angle  $\bar{\theta}$ . The constrained minimization problem associated with the cost (37) in [1] is then numerically solved, resulting to the nominal values for the parameters  $\alpha_s$ ,  $\alpha_r$ , and to the fixed point state  $\bar{x}_s^-$ . The solution of the minimization problem is

$$l_{\text{nat}} = 0.91\text{m}, k_A = 7578.6 \text{ N/m}, k = 7898.4 \text{ N/m}, r_0 = 1.14\text{m}, \Delta r = 0.008\text{m}, \bar{\psi} = 9.7^\circ$$

$$\bar{x} = 0.193 \text{ m}, \bar{y} = 1.129 \text{ m}, \bar{\theta} = 89.6^\circ, \dot{\bar{x}} = 2 \text{ m/s}, \dot{\bar{y}} = 1.33 \text{ m/s}, \dot{\bar{\theta}} = 0 \text{ }^\circ/\text{s}.$$

#### B2) Designing the Virtual Holonomic Constraints in the Rigid Target Model controller:

As is mentioned in the Appendix of [1], the use of Bézier polynomials simplifies the implementation of the conditions for hybrid invariance (conditions (i) and (ii) of Section III C in [1]). One however, could parameterize the holonomic constraints  $h_d$  imposed on the actuated degrees of freedom, see [1] (20), using standard polynomials. Then, the constraints imposed on the leg length and the pitch angle are given by

$$l_d(q_u) = \sum_{j=0}^M \left( \frac{q_u - \mu_1}{\mu_2} \right)^j \tilde{\alpha}_j, \quad (\text{S-2})$$

$$\theta_d(q_u) = \tilde{\alpha}_{M+1}, \quad (\text{S-3})$$

where  $\mu_1$  and  $\mu_2$  are the parameters of a centering and scaling transformation intended to improve the numerical properties of the polynomial, and they will be included in the optimization. Note that, because the primary goal of this work is to compare the Rigid Target Model controller with the SLIP embedding controller to highlight the significance of compliance in transient motions, a constant polynomial was used for the pitch angle. The constrained optimization problem (37), (38) in [1] is then solved with the “search” states being the parameters  $\alpha_s = (\tilde{\alpha}_j)_{j=0,\dots,M+1}$ ,  $\alpha_f = \phi^{\text{td}}$ ,  $\mu_1$ ,  $\mu_2$ , together with the fixed point states  $\bar{x}_s$ . The results of the optimization are presented below

$$\begin{aligned}\tilde{\alpha}_0 &= 0.783, \tilde{\alpha}_1 = 0.003, \tilde{\alpha}_2 = 0.041, \tilde{\alpha}_3 = -0.0001, \tilde{\alpha}_4 = 3.62 \times 10^{-5}, \\ \tilde{\alpha}_5 &= -4.94 \times 10^{-5}, \tilde{\alpha}_6 = -0.0003, \tilde{\alpha}_7 = 1.5655, \mu_1 = 1.574, \mu_2 = 0.124, \\ \bar{x} &= 0.195 \text{ m}, \bar{y} = 1.129 \text{ m}, \bar{\theta} = 89.7^\circ, \dot{\bar{x}} = 2 \text{ m/s}, \dot{\bar{y}} = 1.31 \text{ m/s}, \dot{\bar{\theta}} = 0 \text{ }^\circ/\text{s}.\end{aligned}$$

### C. Achieving Hybrid Invariance

In this section, details regarding the implementation of hybrid invariance are presented. The conditions are easily achievable in the case of the SLIP embedding controller, however, in the case of the Rigid Target Model controller, the addition of the inner loop feedback law  $\Gamma_s$  of Fig. 2 in [1] is necessary.

#### C1) Hybrid Invariance for the SLIP embedding controller

Hybrid invariance in the SLIP embedding controller is a consequence of the form of the flight dynamics of the ASLIP. Indeed, if the ASLIP liftoff occurs when  $\theta = \bar{\theta}$  and  $\ddot{\theta} = \dot{\theta} = 0$ , i.e. on the zero dynamics manifold, then since during flight  $\ddot{\theta} = 0$ , touchdown will occur on the zero dynamics manifold. More details can be found in the proof of Lemma 3 in [2].

#### C2) Hybrid Invariance for the SLIP embedding controller

The easiest way to impose the conditions of hybrid invariance (conditions (i) and (ii) of Section III C in [1]) is to transform the polynomial<sup>1</sup> (S-2) into a Bézier polynomial and apply the rules given in the Appendix of [1]. This section shows how to derive the linear

---

<sup>1</sup> There is no need to update the coefficient of the pitch angle polynomial, since hybrid invariance is achieved through the dynamics of the ASLIP during flight, just as in the case of SLIP embedding controller.

transformation taking the coefficients  $(\tilde{\alpha}_j)_{j=0,\dots,M}$  of the standard polynomial (S-2) into the coefficients  $(\alpha_j)_{j=0,\dots,M}$  of a Bézier polynomial, and vice versa.

Suppose  $[q_u^{\min}, q_u^{\max}]$  is the interval in which  $q_u$  takes its values. Since the degree of the polynomial is  $M = 6$ , take  $N = 5$  points from  $[q_u^{\min}, q_u^{\max}]$  including  $q_u^{\min}$  and  $q_u^{\max}$ . The sampling vector is then  $q = [q]_{i=1,\dots,5}$ , with  $q_1 = q_u^{\min}$  and  $q_5 = q_u^{\max}$ . Evaluate

$$\hat{q}_i = \frac{q_i - \mu_1}{\mu_2}, \quad \dot{\hat{q}}_i = \frac{\dot{q}_i}{\mu_2}, \quad i = 1, \dots, 5, \quad (\text{S-4})$$

$$s_i = \frac{q_i - q^{\min}}{q^{\max} - q^{\min}}, \quad \dot{s}_i = \frac{\dot{q}_i}{q^{\max} - q^{\min}}, \quad i = 1, \dots, 5. \quad (\text{S-5})$$

Equating the standard polynomials with the Bézier polynomials we have

*Positions:*

$$\sum_{j=0}^M [\hat{q}_i^j] \tilde{a}_j = \sum_{j=0}^M \left[ \frac{M!}{j!(M-j)!} s_i^j (1-s_i)^{M-j} \right] a_j, \quad \text{for } i = 1, \dots, 5. \quad (\text{S-6})$$

*Boundary velocities:*

$$\left( \sum_{j=1}^M [j \hat{q}_i^{j-1} \dot{\hat{q}}_i] \tilde{a}_j \right) = \sum_{j=0}^{M-1} \left[ \frac{M!}{j!(M-j-1)!} s_i^j (1-s_i)^{M-j-1} \dot{s}_i \right] (a_{j+1} - a_j), \quad \text{for } i = 1, 5. \quad (\text{S-7})$$

In particular, since  $s_1 = 0$  and  $s_5 = 1$ , in view of properties of the Bézier polynomials, the last two equations for the boundary velocities take the simple form

$$\left( \sum_{j=1}^M [j \hat{q}_1^{j-1} \dot{\hat{q}}_1] \tilde{a}_j \right) = -M \dot{s}_1 a_0 + M \dot{s}_1 a_1, \quad (\text{S-8})$$

$$\left( \sum_{j=1}^M [j \hat{q}_5^{j-1} \dot{\hat{q}}_5] \tilde{a}_j \right) = -M \dot{s}_5 a_5 + M \dot{s}_5 a_6. \quad (\text{S-9})$$

Hence, the following linear system of equations arises

$$L_1 \tilde{a} = L_2 a, \quad (\text{S-10})$$

where

$$(L_1)_{ij} = \hat{q}_i^{j-1}, \quad \text{for } i \in \{1, \dots, 5\}, j \in \{1, \dots, 7\},$$

$$(L_1)_{6,1} = 0, \quad (L_1)_{6,j} = (j-1) \hat{q}_1^{j-2} \dot{\hat{q}}_1, \quad \text{for } j \in \{2, \dots, 7\}, \quad (\text{S-11})$$

$$(L_1)_{7,1} = 0, (L_1)_{7,j} = (j-1)\hat{q}_5^{j-2}\dot{q}_5, \text{ for } j \in \{2, \dots, 7\},$$

and

$$(L_2)_{ij} = \frac{M!}{j!(M-j)!} s_i^j (1-s_i)^{M-j}, \text{ for } i \in \{1, \dots, 5\}, j \in \{1, \dots, 7\}. \quad (\text{S-12})$$

Hence, the linear transformation mapping the coefficients of a standard polynomial  $\tilde{a}$  into the coefficients  $a$  of a Bézier polynomial is

$$a = T(q_u^{\min}, q_u^{\max}) \tilde{a}, \quad (\text{S-13})$$

where

$$T(q_u^{\min}, q_u^{\max}) = L_2^{-1} L_1. \quad (\text{S-14})$$

It is emphasized that the linear transformation  $T(q_u^{\min}, q_u^{\max})$  is a function of  $q_u^{\min}$  and  $q_u^{\max}$ , and therefore to compute it, the values of these parameters must be known. To ensure that liftoff occurs on  $S_{s \rightarrow f} \cap Z_{\alpha_s^+} = S_{s \rightarrow f} \cap Z_{\alpha_s}$  ( $S_{s \rightarrow f} \cap Z_{\alpha_s}$  corresponds to the nominal, i.e. fixed point, values of the stance parameters  $\alpha_s$ )  $q_u^{\max}$  is always selected to be equal to its nominal value. On the other hand  $q_u^{\min}$  is selected to be equal to the current value at touchdown.

To conclude, at each touchdown the coefficients of the Bézier polynomial are updated based on the rule (43) in the Appendix of [1]. Then, we compute  $q_u^{\min}$  based on the values of the state at touchdown, and set  $q_u^{\max}$  equal to its nominal value so that the matrix  $T(q_u^{\min}, q_u^{\max})$  can be calculated. Given  $T(q_u^{\min}, q_u^{\max})$  and the updated values of the Bézier polynomial coefficients, the updated values of the coefficients of the standard polynomial are computed by inverting (S-13).

## II. SIMULATION RESULTS

### A. Recovery from a perturbation

In the paper [1] plots presenting pitch angle, forward velocity, and leg forces as the ASLIP recovers from a perturbation  $\delta\theta = -6\text{deg}$  using both controllers were included. In this supplement more plots are given that support the arguments in [1]. More specifically, the Cartesian trajectory of the COM as the ASLIP recovers from the given pitch perturbation, is given in Fig. 1, while Fig. 2 and 3 present the corresponding leg angle and length during the same motion. Fig. 4 present the hip torque required by the controller, and Figs. 5 to 7 present the horizontal and vertical components of the ground force developed during the motion of the ASLIP, showing that the corresponding constraints are all met.

#### A1) Cartesian variables and Leg states

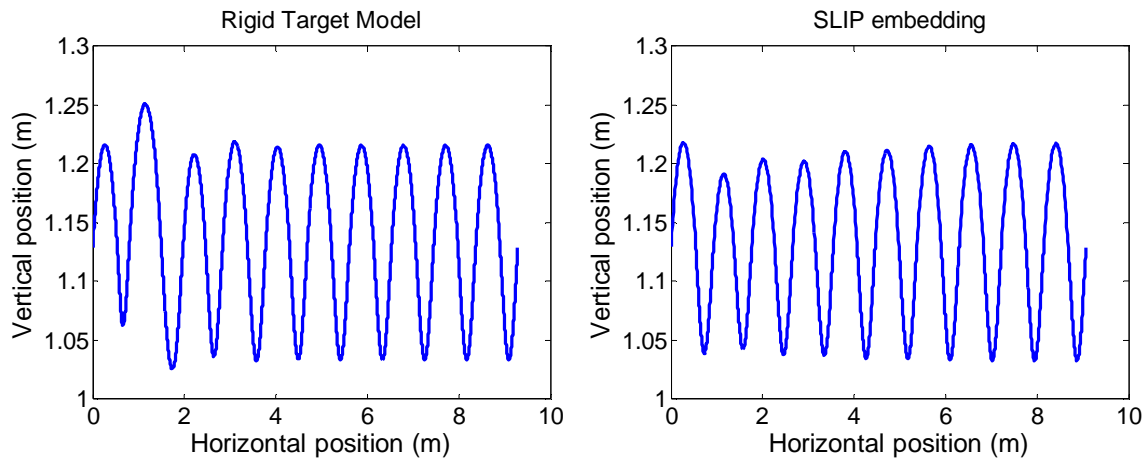


Figure 1. Cartesian trajectory of the COM in recovering from a perturbation  $\delta\theta = -6\text{deg}$ . Left: Rigid Target Model controller; right: SLIP embedding controller.

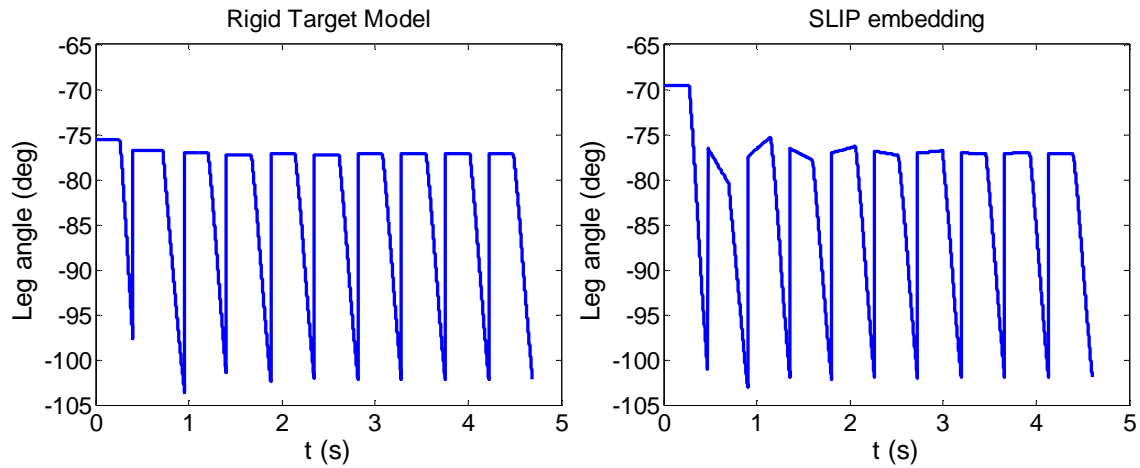


Figure 2. Leg angles. Left: Rigid Target Model controller; right: SLIP embedding controller. Notice that the leg angle in the SLIP embedding is not constant during flight since it is a function of the pitch by (34) in [1]. It is worth mentioning that, at the first step, the leg angle during flight appears to be constant. This is a result of the particular perturbation, for which  $\dot{\theta} = 0$ .

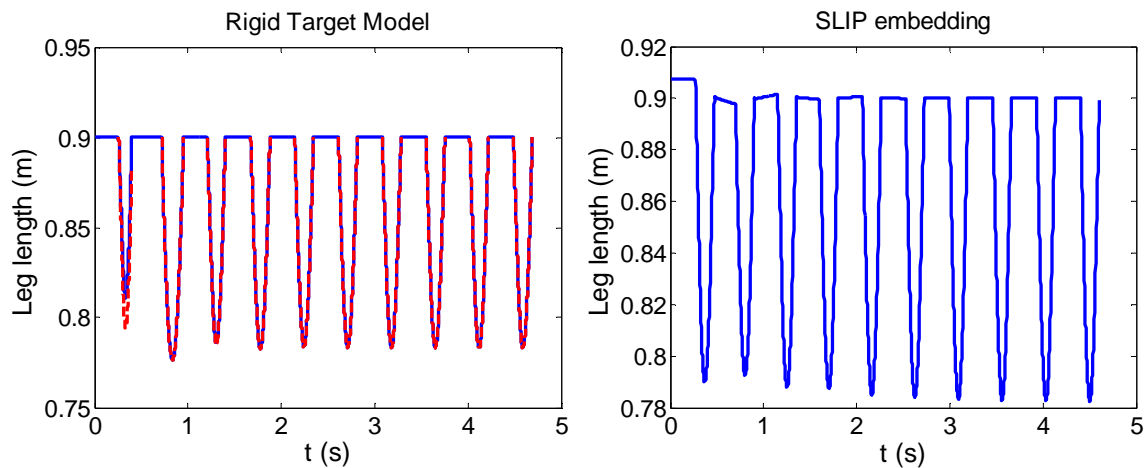


Figure 3. Leg length. Left: Rigid Target Model controller (actual length solid, desired length dashed); right: SLIP embedding controller. Notice again that the leg length in the SLIP embedding during flight is not constant since it is a function of the pitch.

### A2) Continuous Controller Inputs: Hip Torques

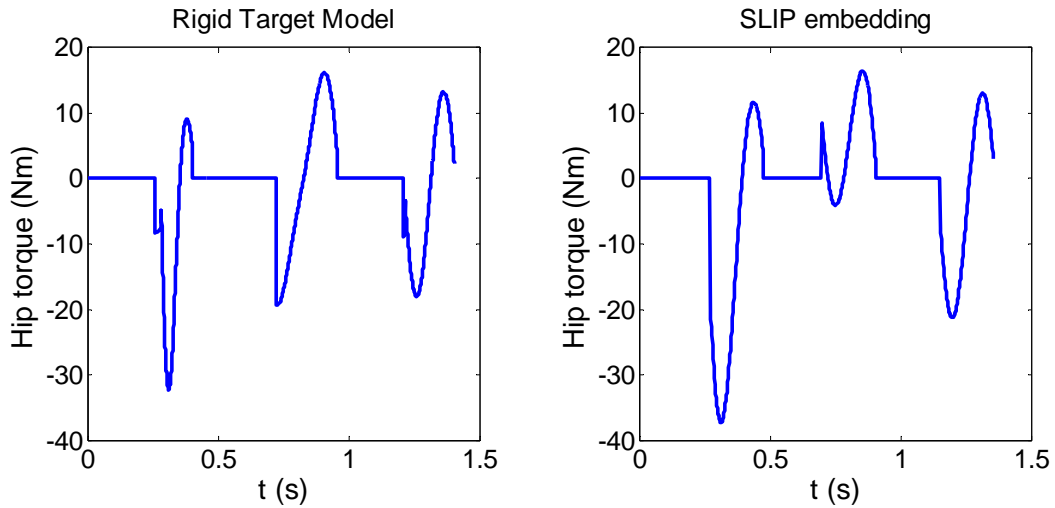


Figure 4. Hip torque. Left: Rigid Target Model controller; right: SLIP embedding controller. Reasonable values in both cases. Note the effect of the saturation in the hip torque developed by the Rigid Target Model controller. Leg forces are detailed in [1], see Fig. 5, and, hence, they are not presented here.

### A3) Ground Reaction Forces

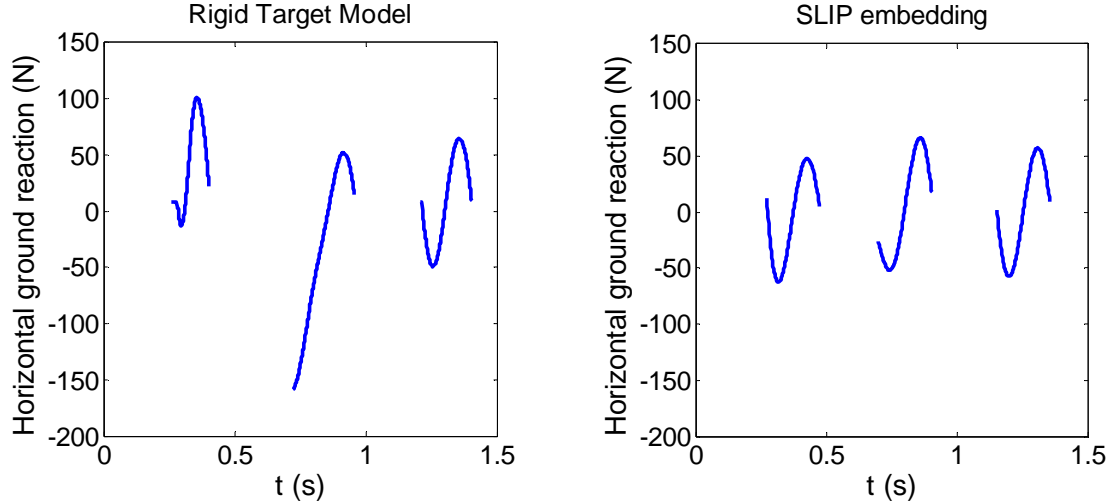


Figure 5. Horizontal ground force component. Left: Rigid Target Model controller; right: SLIP embedding controller. In the SLIP embedding controller, the horizontal ground reaction forces are similar to the SLIP ground reaction forces, even when the system is not on the nominal orbit.

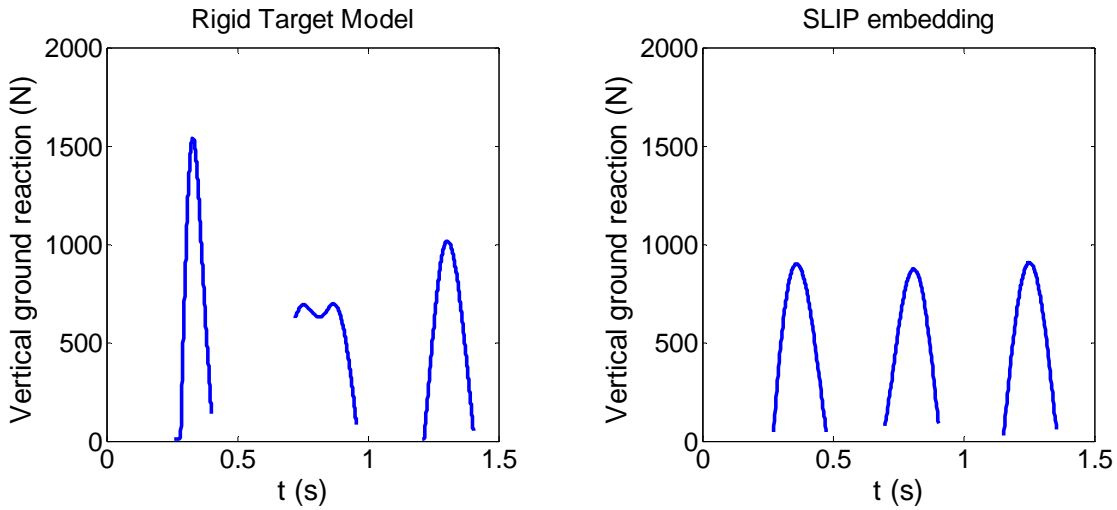


Figure 6. Vertical ground force component. Left: Rigid Target Model controller, right: SLIP embedding controller. The fact that the values are always positive means that the unilateral ground force constraint is not violated (the robot does not pull the ground). Notice that in the Rigid Target Model saturation of the input torques must be used.

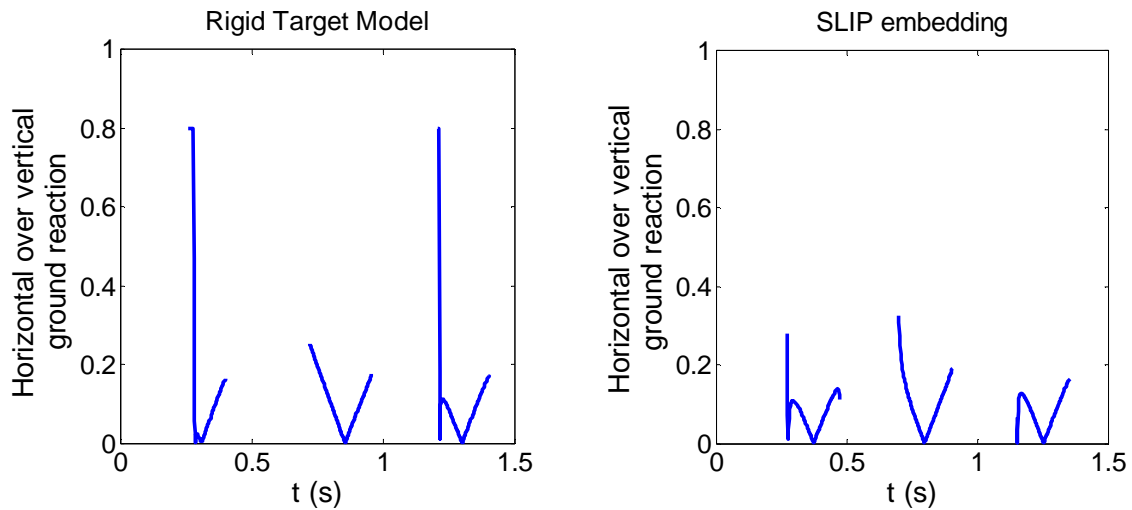


Figure 7. Ratio of the horizontal over the vertical ground force components. Left: Rigid Target Model controller, right: SLIP embedding controller. The friction coefficient is taken to be 0.8 and is never exceeded. This means that no sliding occurs. Again in the Rigid Target Model this is a result of the saturation.

### B. Maximum Perturbations Rejected

The following table complements Table II of [1] with the rest of the states. The perturbations are assumed to enter the system right after liftoff. Perturbations in vertical positions are omitted because they result in the toe “scuffing” the ground. Note also that, in the SLIP embedding controller, no saturation is included. This is the reason why the SLIP controller cannot reject  $\delta\dot{\theta} = -15 \text{ deg/s}$ , which is the magnitude of the perturbation rejected by the RTM controller.

| <b>Perturbation</b>                      | <b>Control</b> | <b>Stride</b> | $(u_1^a, u_2)^{\max}$ | $(W_1, W_2)^{\text{total}}$ |
|--|----------------|---------------|-----------------------|-----------------------------|
| $\delta y = 0.09m$                       | RTM            | 2             | (473, 22.5)           | (34, 9)                     |
|  | SLIP           | 5             | (105, 22)             | (39, 23)                    |
| $\delta\dot{y} = +0.5 \text{ m/s}$       | RTM            | 3             | (468, 23)             | (37, 13.5)                  |
|  | SLIP           | 5             | (92, 22)              | (36, 23)                    |
| $\delta\dot{y} = -2.7 \text{ m/s}$       | RTM            | 5             | (416, 25)             | (55, 22)                    |
|  | SLIP           | 1             | (8, 17)               | (1, 5)                      |
| $\delta\dot{\theta} = +16 \text{ deg/s}$ | RTM            | 7             | (477, 15)             | (83, 27)                    |
|  | SLIP           | 5             | (59, 31)              | (29, 23)                    |
| $\delta\dot{\theta} = -15 \text{ deg/s}$ | RTM            | 4             | (490, 28.2)           | (75, 20)                    |
| $\delta\dot{\theta} = -12 \text{ deg/s}$ | SLIP           | 4             | (51, 30)              | (18, 20)                    |

The following table includes the maximum and minimum perturbations rejected by the SLIP embedding controller respecting all the constraints. In this table saturation is included. It is immediately clear that the domain of attraction is much larger than that of the Rigid Target Model controller results presented in the previous table.

| <b>Perturbation</b>                             | <b>Stride</b> | $(u_1^a, u_2)^{\max}$ | $(W_1, W_2)^{\text{total}}$ |
|---|---------------|-----------------------|-----------------------------|
| $\delta y_{\max} = 0.3m$                        | 6             | (487.3, 32.6)         | (128.5, 28.4)               |
| $\delta\theta_{\max} = +15 \text{ deg}$         | 10            | (214.8, 55.3)         | (85, 53)                    |
| $\delta\theta_{\min} = -19 \text{ deg}$         | 10            | (442, 100)            | (90, 70)                    |
| $\delta\dot{x}_{\max} = +0.9 \text{ m/s}$       | 6             | (415, 16)             | (110, 40)                   |
| $\delta\dot{x}_{\max} = -0.7 \text{ m/s}$       | 8             | (113, 31)             | (56, 35)                    |
| $\delta\dot{y}_{\max} = +1.3 \text{ m/s}$       | 6             | (406, 31)             | (121, 28)                   |
| $\delta\dot{y}_{\min} = -4 \text{ m/s}$         | 6             | (434, 32)             | (88, 28)                    |
| $\delta\dot{\theta}_{\max} = +49 \text{ deg/s}$ | 16            | (256, 51)             | (98, 75)                    |
| $\delta\dot{\theta}_{\min} = -56 \text{ deg/s}$ | 8             | (313, 99)             | (71, 59)                    |

## REFERENCES

- [1] Poulakakis I. and Grizzle J., “Monopedal Running Control: SLIP Embedding and Virtual Constraint Controllers”, *IEEE/ RSJ Int. Conf. on Intelligent Robots and Systems*, under review, 2007.
- [2] Poulakakis I. and Grizzle J., “Formal Embedding of the Spring Loaded Inverted Pendulum in an Asymmetric Hopper”, in *Proc. of the European Control Conference*, to appear, 2007.